DESIGN OF DUAL FREQUENCY INTERFEROMETRIC SAR

Yunjin Kim, Wendy Edelstein, and Ed Caro

Jet Propulsion Laboratory
California Institute Technology
Pasadena, CA911 09
(818) 354-9500

Abstract

Using a spaceborne interferometric SAR, it is possible to produce a high resolution global topographic map with a height accuracy of several meters. However, frequency selection of the interferometric SAR is rather complicated due to interferometric phenomenology and atmospheric effects. In this paper, we propose a dual frequency interferometric SAR to achieve better understanding of interferometric height (especially for penetrable medium) and corresponding calibration and to remove the atmospheric effects. The selected frequencies are L- and Ku-bands. We also present a radar design and show that a light weight and efficient SAR can be designed using new technologies and dual frequency advantages even with two frequency radars in a single spacecraft.

1. INTRODUCTION

SAR (Synthetic Aperture Radar) interferometry demonstrated its capability to generate high resolution topographic maps using two antennas separated in the across track direction (Zebker 1986). Using this technique, it is possible to do a global topographic mission (Zebker 1994). It also was used for velocity mapping of ocean currents when two antennas are separated in the along track direction (Goldstein 1987). In addition to these two fundamental utilities of the interferometric SAR, it also has the potential to provide other scientific findings such as biomass estimation. In this paper, we present a design and advantages of a dual frequency interferometric SAR. The primary purposes of having two frequencies are to obtain better phenomenological understanding and interferometric calibration for height accuracy improvement, We proposed to use an L- and Ku- band pair for the dual frequency radar.

A dual frequency interferometric SAR has many advantages over its single frequency counterpart. First, the L-band interferometric SAR may not be able to collect data over high latitude areas because the baseline, formed by the two separate spacecraft, is not sufficient] y long at high latitudes. However, the Ku-band interferometer, which has a fixed baseline within a single spacecraft, can take data without this restriction. The second advantage is better understanding of interferometric phenomenology. The meaning of interferometric height is not clearly defined when the imaged area is composed of RF penetrable media (snow, sand, and tree). As an example, the interferometric tree height is very sensitive to the radar frequency. A lower frequency signal penetrates deeper into the canopy and the interferometric height is closer to the ground. In addition, the depth of the penetration depends on the density of the canopy. If we use a dual frequency radar (I.- and Ku-band), the tree height difference of two frequency data may provide a way of calculating the tree top location. In addition, this difference information can be very useful for biomass estimation. The third advantage is to remove atmospheric effects on the interferometric data using two frequencies. Since the L-band signal is less sensitive to the weather condition, the L-band interferometric SAR provides better all weather capability. On the other hand, the L-band signal suffers more ionospheric disturbance which causes a signal delay (both common and differential) and Faraday rotation. Using a circularly polarized antenna, the

Faraday rotation effects can be eliminated. However, to remove the ionospheric effects, TEC (Total Electron Content) should be estimated. This TEC estimation process can bc done using both L- and Ku-band data and the signal delay effects on the L-band data will be compensated. The fourth advantage is to relax the metrology requirements on the Ku-band system by using the L-band topographic map. The slowly varying metrology error results in tilt of the topographic map. Since the L-band system measures the baseline vector using highly accurate differential GPS, the L-band topographic map can be used as tie points for the Ku-band interferometric map.

2. MISSION DESCRIPTION

The mission goals are listed in Table 1. The L-band system is composed of two spacecraft, flying in tandem, separated by less than 2 km. The Ku-band system requires a single spacecraft (shared with one of the L-band radars) with the fixed baseline length of 60 meters.

Table 1. Mission goals.

Height Accuracy	better than 5 meters
Resolution	30 m x 30 m
Mission Duration	3-5 years

The maximum L-band baseline length is determined based on the ground phase change rate. For Ku-band, the baseline length is limited by the length of the boom realizable. The spacecraft orbit is a sun-synchronous, circular orbit with an altitude of 565 km. This altitude was chosen to balance the SNR loss due to slant range increase and differential drag of the twin spacecraft. Since the orbit repeats every 84 days, the swath size should be larger than at least 32 km. This interferometric mission is composed of two phases. During the first phase, we map the topography of the entire land mass using both L- and Ku-band system simultaneously. Then, during the second phase, the L-band spacecraft will align in the along track direction and gather velocity mapping data over ocean and coastal areas. In this second phase, each radar also collects data over land (selected sites) to form differential interferometric images to detect minute land motion,

3. INSTRUMENT SYSTEM DESCRIPTION

The radar system is designed based on the parameters listed in Table 2. The radar instrument is composed of the antenna subsystem and the sensor electronics. The sensor electronics consists of the RF electronics which transmits and receives the radar signals and the Digital electronics which includes the data handling system, control and timing unit and system power distribution.

3-1. Antenna Subsystem

The antenna subsystem consists of three individual planar arrays, where each antenna uses a conventional architecture, such as microstrip for L-band and slotted waveguide for Ku-band. The baseline for the Ku-band system is formed by a 60 meter deployable boom. For maximum sensitivity, low noise amplifiers will be distributed along each array. To compensate for the long path loss on the second Ku-band (receive only) antenna, additional low noise amplifiers will be distributed along the boom or an optical modulator will be implemented so that very low loss fiber can be used for the signal return.

Table 2. Radar parameters of the proposed dual frequency interferometric SAR.

Radar Parameter	L-band	Ku-band
Wavelength	0.24 m	0.02 m
Look angle	35 deg.	35 deg.
Antenna size	8 m x 3.5 m	8 m x 0.3 m
Polarization	Circular	VV
Peak transmit power	1600 W	2100 W
Bandwidth	25 MHz	25 MHz
Pulse length	50 µsec	50 µsec
PRF (nominal)	2150 Hz	2150 Hz
Duty Cycle (nominal)	10.75 %	10.7590
Sampling frequency	60 MHz	60 MHz
Swath size	40 km	40 km
Data rate (per channel)	109 Mbits/sec	109 Mbits/sec

Another antenna approach utilizes an inflatable parabolic reflector antenna. Inflatable antennas offer a potentially significant savings in mass and volume compared to rigid antennas of equivalent aperture size. Using an inflatable reflector, with three feeds, both L- and Ku- band can share the same radiating surfaces, where the Ku-band baseline is formed by partially illuminating opposite sides of the reflector. In this way, significant volume and mass savings can be realized. The main disadvantage to this approach is that current inflatable technology limits the antenna diameter to about 30 meters which would severely limit the performance.

3-2. R F Electronics Subsystem

The RF Electronics Subsystem (RFES) consists of three major functional blocks - the Exciter, the Transmitters and the Receivers. The hardware elements of the Exciter include a frequency reference source, a linear FM modulator, frequency translators to L-band and Ku-band, and driver amplifiers, A crosslink transceiver synchronizes radar timing signals between the twin spacecrafts. By sharing common exciter elements, the L-band and Ku-band pair can be realized on a single spacecraft at a relatively low mass and power consumption. The excitation signal is generated at baseband using a Numerically Controlled Oscillator (NCO) based digital chirp generator which generates chirps with 25 MHz bandwidth and 50 µsec pulsewidth. This baseband signal is then frequency translated to L.-band and Ku-band and the resulting signals are then amplified to the level required by the transmitter using solid-state power amplifiers. The clock frequencies, local oscillator frequencies, and the system timing signals are derived from a crystal oscillator reference. All technologies in the Exciter are mature, although some elements, such as the high-speed NCO, may require some custom engineering design to qualify the packaging for space.

The transmitters amplify the L-band and Ku-band output of the upconverter/driver to the level required at the feed. Each transmitter also includes a power combiner to sum the outputs of the amplifier modules and a circulator to diplex the transmit and receive signals. For both L-band and Ku-band, multiple units will be coherently combined. The L-band transmitter consists of eight 200 Watt solid-state power amplifiers (SSPA) for a total of 1.6 KWatts delivered to the antenna feed (less circulator, cable and feed losses). SSPA technology at L-band is mature, where 200 Watt silicon bipolar power devices are readily available. The Ku-band transmitter consists of seven 300 Watt Microwave Power Modules (MPM) for a total of 2.1 KWatts delivered to the antenna feed (less circulator, cable and feed losses). MPM technology combines a miniaturized helix TWT driven by a MMIC solid state power amplifier in a small package with integrated power conditioning. Each unit delivers about 300 Watts with 50 dB of gain at 40% efficiency.

The MPM is more reliable, efficient and smaller than the conventional TWT at a significantly more affordable cost. Development of MPMs has been underway for several years, although this technology is still far less mature than solid-state or conventional TWT. Current efforts are being made to qualify the MPM for space applications as well as demonstration of the power combining capability.

The receive signal is amplified and coherently downconverted to offset video in the Receiver. The input of the Receiver is protected against overdrive from transmitter leakage by a limiter, which is followed by a low noise amplifier. Gain control is used to optimize system dynamic range and simplify radar operation. The radar electronics will take advantage of advances made in the MMIC industry by implementing hybrid and monolithic integrated circuit technology for a significant reduction in the mass, power and volume of the radar sensor electronics.

3-3. Digital Electronics Subsystem

The Digital Electronics Subsystem consists of three functional blocks — the Data System, the Control and Timing Unit and Power Distribution. The Data System receives the video signals from each of the three receiver channels and digitizes the data using an 8-bit ADC, sampling at 60 MHz, The buffer slows down the data rate and the data is then reduced from 8-bits to 4-bits using Block Floating Point Quantization (BFPQ). The high-speed formatter and data multiplexer converts the data from parallel to serial format and transfers it with header information to the spacecraft on-board data recorders. The radar science data is downlinked by the spacecraft X-band link.

The Control and Timing Unit interfaces with the spacecraft computer which stores and executes commands and monitors radar telemetry. The spacecraft S-band link is used for command uplink and telemetry downlink. The timing electronics receive the reference clock frequency from the RFES and generates all required radar timing signals. High-density field programmable gate array (FPGA) technology will be implemented in the digital electronics for significant mass and power reduction.

The Power Distribution unit is the main power source for the radar instrument. The power electronics filters the raw 28 VDC spacecraft power and derives and distributes all required DC voltages utilizing light-weight, high-efficiency, high-density power supplies.

A block diagram of the proposed radar instrument for a single satellite is shown in Figure 1. By combining multiple transmitter modules, a transmitter failure will gracefully degrade the radar performance. These transmitters could also be integrated with the low noise amplifier into a Transmit/ Receive (T/R) module and distributed along the array, where one T/R could drive a single panel. This would eliminate additional path losses and thus further improve system performance. There is one L-band and two Ku-band receive channels all operating simultaneously and coherently.

The instrument mass is roughly 250 Kg and the DC power usage is about 1,6 KW in full multifrequency interferornetric operation. Details of the instrument mass and power budget is provided in Table 3. The L-band transmitters assume 1.6 KW of peak transmit power at 10.75% duty cycle with 40% efficiency. The Ku-band transmitters assume 2.1 KW of total transmit power at 10.75% duty cycle with 40% efficiency.

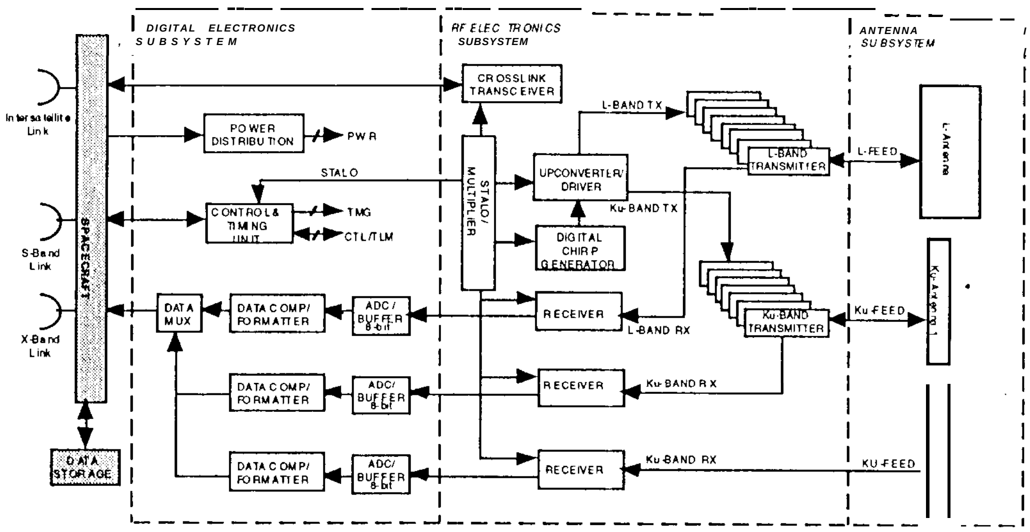

Figure 1 — Instrument Block Diagram

Table 3- Instrument Mass & Power Estimates

	Mass	Power
Antenna Subsystem	**192 Kg**	**7 W**
L-Band Antenna Panels (8)	50	0
Ku-Band Antenna Panels (8x2)	43	0
Distributed Low Noise Amps	7	7
Antenna Structures (3)	60	0
Corporate Feed Network (3)	22	0
Deployment Mechanisms	10	0
RF Electronics Subsystem	**40 Kg**	1089 W
L-Transmitter (8x200W, 40% eff)	12	430
Ku-Transmitter (7x300W, 40% eff)	18	564
Exciter (STALO, Chirp Generator, Crosslink)	3	60
Upconverter/Driver	2	20
L-Band Receiver (1 unit)	1	5
Ku-Band Receiver (2 units)	2	10
Housing & Cabling	2	0
Digital Electronics Subsystem	**23 Kg**	**480 W**
Control & Timing Unit	2	23
ADC/Buffer (3 channels)	6	54
Data Compressor/Formatter (3 channels)	6	120
Data Multiplexer	2	20
Power Distribution (80% conv eff)	5	263
Housing & Cabling	2	0
Instrument Total	**2.54 Kg**	**1576** W

3-4. Attitude Determination Subsystem

The interferometric baseline knowledge must be updated frequently to ensure high accuracy topographic maps. For L-band, a differential GPS is used to measure the baseline with an accuracy of 1 mm (90 %). For Ku-band, an attitude transfer and range finder metrology system measures the baseline length and attitude. The spacecraft attitude is measured using a 2 arcsec (1 σ) star tracker even though the metrology requirements on the Ku-band system can be relaxed by using the L-band topographic map as tie points.

4. PERFORMANCE ESTIMATION

Since the baseline length of the L-band interferometric SAR changes, the height accuracy suffers latitude dependent variation. For the baseline length of 670-2000 m for L-band and 60 m (90 degrees boom orientation) for Ku-band, Table 4 summarizes the height accuracy based on standard error analysis methods (Li 1990, Rodriguez 1992).

Table 4. Estimated height accuracy of the proposed dual frequency interferometer. The height accuracy in () represents the Ku-band error using L-band topographic map as tie points.

Error Source	L-band	Ku-band
Phase Noise	1. 0 - 2.0 m	3.0 m
Baseline Knowledge	0.5 m	4.5 m (0.5 m)
Atmosphere	0.5 m	0.3 m
Others	1.0 m	1.0 m
RSS	1.6- 2.4 m	5.5 m (3.2 m)

The Ku-band relative accuracy can be improved significantly by increasing the baseline length. The Ku-band height error due to the metrology can be reduced by using tie points obtained from the L-band topographic map. For the velocity mapping (along-track interferometry), with 700 meters spacecraft separation, the L-band interferometer provide the velocity accuracy of around 8 cm/sec for 100 m x 100 m resolution.

5. CONCLUSIONS

We discussed the advantages of a dual frequency interferometric radar in terms of area coverage, phenomenology, atmospheric error removal, and data calibration. We presented a design and performance of a L- and Ku- band dual frequency interferometric SAR. The L-band height accuracy is 2-3 m while Ku-band accuracy is approximately 3 -4 m with L-band tie points. The Ku-band performance can be improved by using longer baseline.

Acknowledgment

The research described in this paper was carried out by the Jet Propulsion Laboratory under contract with the National Aeronautics and Space Administration.

References

Goldstein, R. M., and H. A. Zebker, "Interferometric radar measurement of ocean surface current," Nature, 328, 707-709, 1987.
Li, F., and R. M. Goldstein, "Studies of multi-baseline spaceborne interferometric synthetic aperture radars, " IEEE Trans. Geosci. Remote Sensing, 28, 88-97, 1990.
Rodriguez, E., and J. Martin, "Theory and design of interferometric synthetic aperture radars," IEE Proceedings, 139, 147-159, 1992.
Zebker, H. A., and R. M. Goldstein, "Topographic mapping from interferometric SAR observations, " J. Geophys. Res., 91, 4993-4999, 1986.
Zebker, 11. A., T. G. Farr, R, P. Salazar, T.H. Dixon, "Mapping the worlds topography using radar interferometry - The TOPSAT mission," IEEE Proceedings, 82, 1774-1786, 1994.